UAV-BORNE GPR SNOWPACK STRATIGRAPHY

Anna Siebenbrunner[1,2,*], Robert Delleske[3], Markus Keuschnig[3]

[1]Lo.La Peak Solutions GmbH, Innsbruck, Austria
[2]Faculty of Geo- and Atmospheric Sciences, University of Innsbruck, Austria
[3]GEORESEARCH Forschungsgesellschaft mbH, Puch-Urstein, Austria

ABSTRACT: Current methods of snowpack stability assessment primarily rely on professional observations, mainly digging a snow pit. This technique has spatial limitations, is time-consuming, and places observers at risk. The combined usage of UAVs and GPR is capable of providing detailed snowpack layering data at scale without human exposure to potential avalanche-prone areas. The presented study aims to obtain radargrams of the study area's internal snowpack layering structure. A single-channel GPR with a 1000 MHz shielded antenna is attached to a UAV to survey the snowpack. The UAV flights are carried out semi-automatically from a safe spot at a speed of 1 m/s at a LiDAR altimeter-adjusted distance to the snow surface of 5 m. The data obtained by the GPR is then compared to density measurements and manual snowpack observations following international standards. The preliminary results indicate the success of the UAV's flight performance and the accuracy of the GPR data in determining the snow depth and detecting the most prominent layers of the snowpack.

Keywords: snowpack monitoring, GPR, UAV, avalanche hazard assessment

1. INTRODUCTION

Over the years, avalanche professionals have developed methods to investigate the snowpack and assess the avalanche danger. Conventional methods involve digging a snow pit and performing stability tests, entailing multiple disadvantages: They require human exposure to avalanche-prone terrain (Eckerstorfer et al., 2016; Schweizer et al., 2015), are time-consuming and thus costly, and not feasible to representatively cover larger areas (Forte et al., 2012). To overcome the above-mentioned limitations, methods of remote sensing can be applied (Eckerstorfer et al., 2016; Forte et al., 2012). The combined usage of a remotely piloted Unmanned Aerial Vehicle (UAV) and a Ground Penetrating Radar (GPR) has the potential to acquire detailed snowpack layering data (Instanes et al., 2004; Jenssen et al., 2016).

Traditional GPR systems have already been used in the past to detect avalanche victims buried under the snow (Instanes et al., 2004; Keuschnig, 2010), to measure snow depth (McGrath et al., 2019), Snow Water Equivalent (SWE) (Gubler and Hiller, 1984; Holbrook et al., 2016) and Liquid Water Content (LWC) (Schmid et al., 2015), and to investigate the layering structure of the snowpack (Gubler and Hiller, 1984; Holmgren et al., 1998; Sand and Bruland, 1998; Lundberg et al., 2006; Heilig et al., 2008; Schmid et al., 2014). Applying UAV-mounted GPR for snowpack investigations has only been made possible by recent technological progress, thus, studies using UAV-borne GPR are still rare, e.g., Jenssen et al. (2016); Prager et al. (2022); Valence et al. (2022), who conducted their studies on flat terrain. The presented study centers on high-alpine steep terrain, representing a novel contribution to this particular field.

*Corresponding author address:
Anna Siebenbrunner, Lo.La Peak Solutions GmbH,
Holzgasse 18, 6020 Innsbruck;
email: anna@lo-la.info

2. METHODOLOGY

This study aims to investigate the layer structure within an alpine snowpack using UAV-borne GPR. Specific emphasis is dedicated to automating boundary layer detection. This is considered vital for potential operational applications where quick achievement of results is essential. In this work, the GPR-derived results are compared to the *in situ* reference measurements to assess the feasibility of this method in providing a detailed representation of the snowpack's layering structure.

2.1. Research Design

An incremental development process was employed, guided by continuous falsification and verification of intermediate results (see Figure 1). This analytical approach is particularly suitable due to the limited existing knowledge regarding the representation of the snowpack and its failure-relevant weak layers in a radargram.

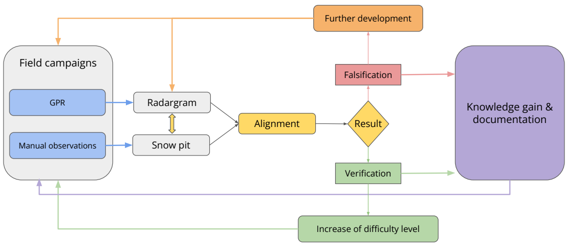

Figure 1: Overview of the methodological approach employed in this study.

2.2. Data Acquisition

Data were acquired in a field campaign in April 2023 at the Kitzsteinhorn glacier ski resort, Austria. A DJI M300 UAV with a 1000 MHz GPR attached was piloted remotely at a constant flight speed of 1 m/s to record GPR data on a pre-defined grid. The flight altitude of the UAV was kept constant at 5 m above the snow surface using a LiDAR altimeter. Additionally, snow depth was probe-measured at 23 points, and three extensive snow pits were dug as reference measurements. The snowpack observations included density and temperature measurements, grain form and size, hand hardness, wetness, and stability tests.

2.3. Data Processing

GPR and reference data had to be processed separately. Snow depth measurements were stored as `.csv` files including geographic coordinates and the corresponding snow depth value. The snowpack observations were noted on paper in the field, thus had to be digitized to be used for the GPR data validation subsequently. The raw GPR data (stored as `SEG-Y`) had to undergo a sequence of pre-processing steps, to allow for detecting the top and bottom snowpack layers in the data. The pre-processing mainly involved filter application (e.g., mean filter, Singular Value Decomposition (SVD), Wiener filter) and data cleaning, i.e., removing useless parts of the data (e.g., turns) and the creation of subsets to ease further processing. At this level of processing, boundary layer detection was possible by employing Computer Vision techniques, such as thresholding. The location of the top and bottom layers was then used to calculate the snow depth and derive the stratigraphy, and consequently compare the GPR-derived data to the *in situ* measured data. The whole workflow is shown in Figure 2. Example results of this algorithm, i.e., detected top and bottom snow layers, are shown in Figure 3.

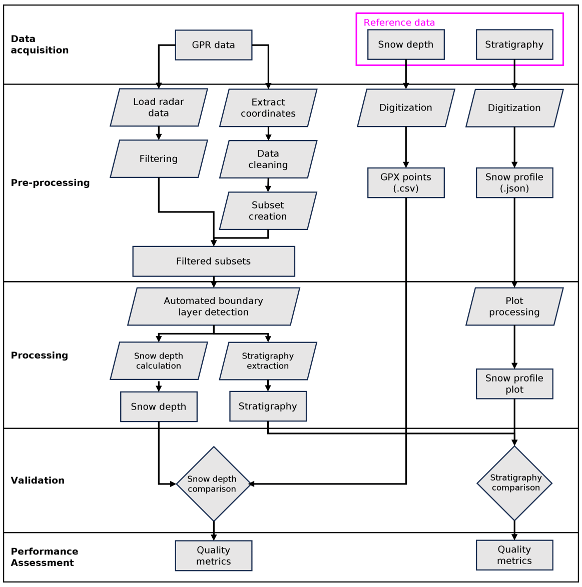

Figure 2: Developed workflow for processing and validation of GPR and *in situ* data.

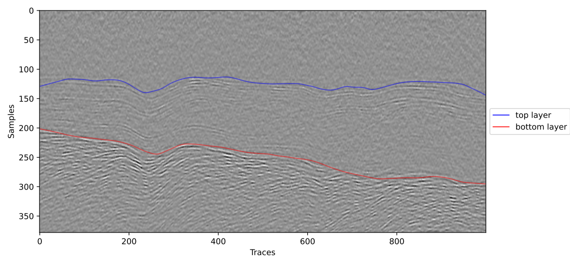

Figure 3: Results of the top and bottom snow layer detection algorithm for one selected subset of 1000 traces. The smoothed estimates are displayed on pre-processed data.

3. VALIDATION OF PRELIMINARY RESULTS

The validation was carried out twofold: (1) as a quantitative comparison of calculated to *in situ* measured snow depth using selected performance metrics and (2) as a qualitative alignment of GPR-derived snowpack stratigraphy and manual snow pits.
To objectively assess the quality of these results, Root Mean Square Error (RMSE), Weighted Root Mean Square Error (WRMSE), Mean Absolute Percentage Error (MAPE), and Pearson correlation coefficient (r), including the p value describing the significance, are used.

3.1. Snow Depth

As for the validation, the calculated snow depth values are regarded as *predicted values*, and compared to the *observed values*, i.e., probe-measured snow depth. During the field campaign, it was aimed to collect *in situ* data in close proximity to the UAV

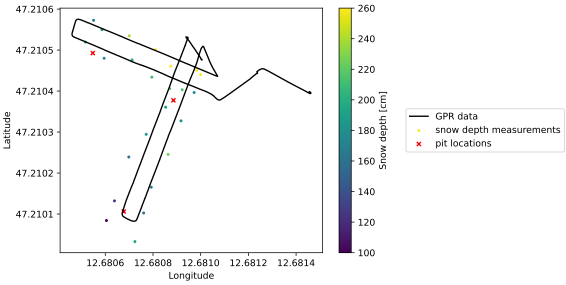

Figure 4: GPR path and locations of snow pits and snow depth measurements.

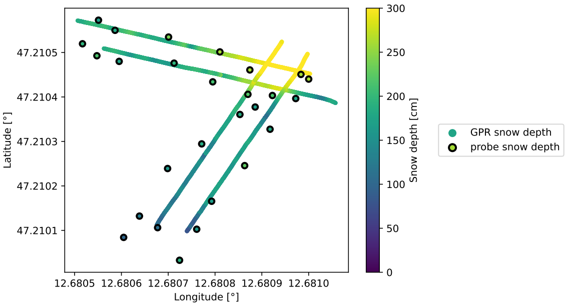

Figure 5: GPR-derived vs. probe-measured snow depth.

flight path. Figure 4 presents the *in situ* data relative to the flight path.

To visually compare the calculated snow depth to the probe-measured values, a color map is shown in Figure 5. It has to be noted that the observed values in the upper right corner may largely deviate from reality because the probe, measuring 2.60 m, was not long enough for the amounts of snow in this specific micro-region.

Table 1 lists the aforementioned performance measures for the comparison of probe-measured and GPR-derived snow depth. The correlation of predicted and measured values is shown in Figure 6.

Table 1: RMSE, WRMSE, MAPE, and Pearson correlation coefficient (r) for observed vs. predicted snow depth concerning the third field campaign at Kitzsteinhorn.

Performance metrics	**Values**
RMSE	29.97 cm
WRMSE	24.90 cm
MAPE	12.20 %
r	0.70
p	0.00064

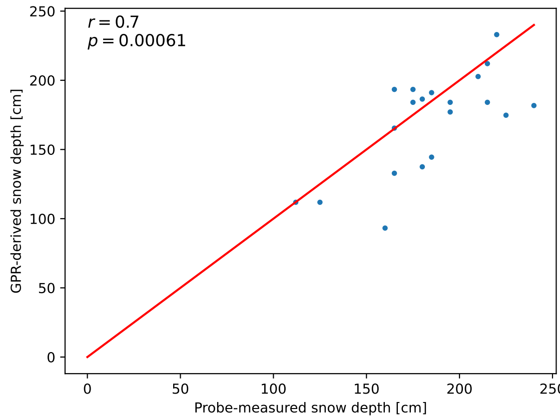

Figure 6: Correlation of GPR-derived and probe-measured snow depth. The red line indicates perfect correlation (1.0).

3.2. *Snowpack Stratigraphy*

Figure 4 shows the location of the three snow pits (displayed as red crosses) relative to the GPR traces that were used for the comparison to the GPR-derived stratigraphy. For these three locations, specific subsets of 1000 traces, where the pit coordinates represent the middle trace of the subset, are created. The three samples differed in snow depth as well as in the internal layering structure. Hence, all three pits had to be evaluated separately. The results of the stratigraphy comparison are discussed in subsection 4.1.

4. DISCUSSION

This section discusses the results of the validation including the performance metrics used. The validation results are then compared to existing related research, and the strengths and limitations of the current state of the methodological approach are elaborated on.

4.1. *Model Performance Assessment*

While the snow depth validation showed – considering the additional difficulty inherent to the complex terrain – promising results, it is obvious that the snowpack stratigraphy derived from the GPR-data is not yet mature enough for operational use and still needs improvement. Still, the most prominent features of the snowpack are observable.
For pit 1.3.1 the top and bottom layer are detected correctly, however, not for the other two pits (see Figure 7a). For pit 1.3.2, the top layer is missed, instead, a harder internal layer is mistakenly detected as top layer (see Figure 7b). This might be due to the top layer being very soft at this location. For

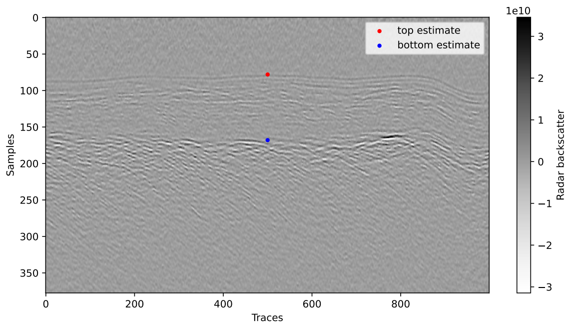

(a) 1.3.1

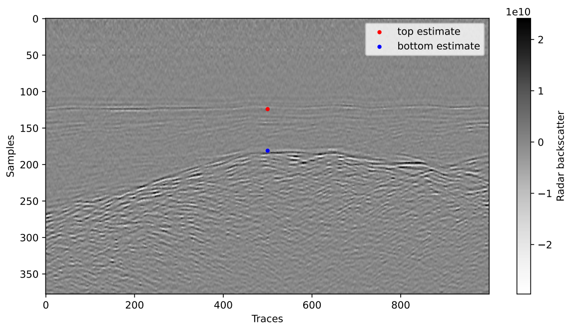

(b) 1.3.2

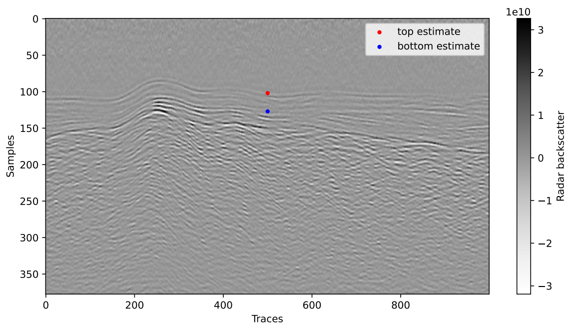

(c) 1.3.3

Figure 7: Detected top and bottom layer for snow pit 1.3.1, 1.3.2, and 1.3.3 acquired at Kitzsteinhorn.

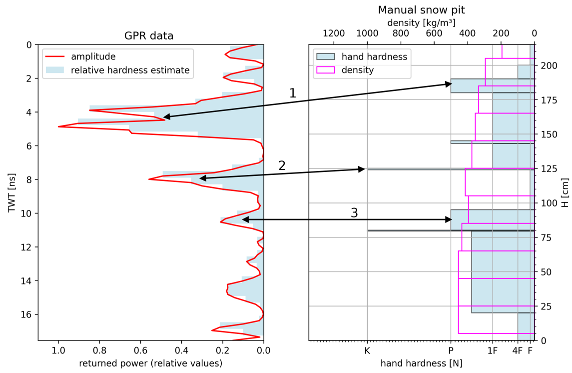

Figure 8: Comparison of GPR data to manual stratigraphy. Horizontal bars (light blue) are inserted to make the comparison to the conventional snow profile plot easier. In the right-hand plot of all the following figures, the manual snowpack stratigraphy based on hand hardness and density measurements is shown. For this pit, hard layers are also visible in the GPR data (see arrows 1-3). This applies also to the majority of the soft layers, e.g., the soft layer between the two harder ones marked by arrows 2 and 3. However, it is clearly visible, that the depiction is not accurate due to attenuation loss in the radar data. Hence, hard layers further down in the snowpack are not perceived as hard layers in the GPR data.

the third pit 1.3.3, a very hard internal layer (presumably ice) is wrongly detected as bottom layer (see Figure 7c), leading to a drastic reduction of the snow depth, and consequently a distorted depiction of the snowpack stratigraphy. All three pits are then compared to the amplitude of the GPR trace closest to the profile location. The most important features (e.g., hard layers) are also well visible in the GPR data. The overall agreement is seen in rudimentary form but still differs to a large degree.

Exemplarily, the comparison for pit 1.3.1 is shown in Figure 8. However, it has to be noted that manual snow pit observations come with a high level of subjectivity and further lack spatial resolution, which makes a direct comparison even harder. Therefore, further evaluation is not considered useful in this case, instead, it is aimed to acquire reference measurements in both higher quantity and quality in the upcoming field campaigns.

4.2. Comparison to Related Work

Previous studies showed an overall good correlation between GPR-derived snow depth and *in situ* measurements using the probe. Prager et al. (2022) compared their UAV-borne GPR data to ground-measured GPR-derived snow depth. They achieved good correlation for the meadow area

(r=0.88), and slightly worse correlation for the forest area (r=0.61), which is likely due to the forest being a more inhomogeneous terrain compared to a meadow. UAV-borne GPR surveys high-alpine, steep terrain, as it was used for investigation in this work, have not yet been reported on by the scientific community. Such complex terrain can be considered even more challenging, which also needs to be taken into account in the comparison of quality metrics to related studies. Therefore, the achieved correlation results and deviations (e.g., RMSE) can be regarded as satisfying in view of the challenging terrain.
Due to the scarcity of existing research in this specific area and the difficulty in applying quality metrics, the comparison of the qualitative validation results of the snowpack stratigraphy to previous work is difficult. Jenssen et al. (2020) and Jenssen and Jacobsen (2020) compared their GPR data acquired on almost flat terrain to their *in situ* stratigraphy. They observed good alignment, especially for the upper part of the snowpack. For steep terrain, the stratigraphy investigation is considered more challenging.

4.3. Strengths and Limitations of the Approach

The major advantage of the presented approach is that data are acquired at areal scale, thus allowing for a more thorough assessment of a whole terrain chamber. Previously, only point scale measurements have been possible relying on conventional snowpack observation methods (e.g., snow pits), which are furthermore considerably slower at data acquisition compared to the UAV. Using the UAV-based approach, snow professionals do not need to expose themselves to hazardous terrain as the UAV can be piloted remotely from a safe spot. The automated boundary layer detection allows for near-real-time results, presuming sufficient computational capacity is available. The developed processing workflow can furthermore be customized according to specific research aims as it is independent of proprietary software.

Given the short period of testing and development so far, the approach is not yet mature for operational application. To further improve the efficiency and reliability of the method, more field campaigns are required in the near future. Here, special attention should be dedicated to increasing the number of reference measurements to allow for extensive evaluation.

5. CONCLUSIONS AND OUTLOOK

Current methods of snowpack monitoring mainly rely on fieldwork, coming along with several disadvantages, such as high resource expenditure. The combination of UAV and GPR has the potential to overcome the limitations of fieldwork, contributing to safer and more efficient data acquisition. The developed algorithm for automated boundary layer detection enables rapid and accurate determination of the current snow depth and derivation of the snowpack stratigraphy. The validation of the method was carried out by comparing the GPR-based snow depth to probe-measured reference data, showing good correlation: r=0.70 (p=0.00061), MAPE=12.20%. The analysis of the stratigraphy data indicates that the adopted approach is technically capable of examining significant components of the snowpack, such as very hard or soft layers, which play a major role in the formation of slab avalanches.

To further refine the presented approach more field campaigns are needed as enhancing the data quantity is expected to improve the approach's quality and thus get it ready for operational usage. Concerning the data processing method, Deep Learning and Machine Learning techniques have the potential to improve the accuracy and efficiency of the approach, as related work by Li et al. (2020); Wang et al. (2022); Dou et al. (2017); Wunderlich et al. (2022); Lei et al. (2019) demonstrated. As the developed approach can be easily adapted, it is possible to apply it, e.g., in the context of glacier or permafrost research, where accurate delineation of boundary layers is also relevant.

ACKNOWLEDGEMENT

The STRATIFY project received financial support from the FFG. The authors thank everyone who helped with the field work.

REFERENCES

Dou, Q., Wei, L., Magee, D. R., and Cohn, A. G.: Real-Time Hyperbola Recognition and Fitting in GPR Data, IEEE Transactions on Geoscience and Remote Sensing, 55, 51–62, doi: 10.1109/TGRS.2016.2592679, 2017.

Eckerstorfer, M., Bühler, Y., Frauenfelder, R., and Malnes, E.: Remote sensing of snow avalanches: Recent advances, potential, and limitations, Cold Regions Science and Technology, 121, 126–140, doi:10.1016/j.coldregions.2015.11.001, URL https://www.sciencedirect.com/science/article/pii/S0165232X15002591, 2016.

Forte, E., Pipan, M., and Colucci, R. R.: GPR velocity and amplitude analyses to characterize the stratigraphy and estimate the ice density: An example from the Eastern Glacier of Mt. Canin (Alpine Chain, Italy), in: 2012 14th International Conference on Ground Penetrating Radar (GPR), pp. 646–652, doi:10.1109/ICGPR.2012.6254942, 2012.

Gubler, H. and Hiller, M.: The use of microwave FMCW radar in snow and avalanche research, Cold Regions Science and Technology, 9, 109–119, doi:10.1016/0165-232X(84)90003-X, URL https://www.sciencedirect.com/science/article/pii/0165232X8490003X, 1984.

Heilig, A., Schober, M., Schneebeli, M., and Fellin, W.: Next Level for Snow Pack Monitoring in Real-Time Using Ground-Penetrating Radar (GPR) Technology, Proceedings Whistler 2008 International Snow Science Workshop September 21-27, 2008, p. 111, URL https://arc.lib.montana.edu/snow-science/item.php?id=18, 2008.

Holbrook, W. S., Miller, S. N., and Provart, M. A.: Estimating snow water equivalent over long mountain transects using snowmobile-mounted ground-penetrating radar, GEOPHYSICS, 81, WA183–WA193, doi:10.1190/geo2015-0121.1, URL https://library.seg.org/doi/10.1190/geo2015-0121.1, 2016.

Holmgren, J., Sturm, M., Yankielun, N. E., and Koh, G.: Extensive measurements of snow depth using FM-CW radar, Cold Regions Science and Technology, 27, 17–30, doi:10.1016/S0165-232X(97)00020-7, URL https://www.sciencedirect.com/science/article/pii/S0165232X97000207, 1998.

Instanes, A., Lønne, I., and Sandaker, K.: Location of avalanche victims with ground-penetrating radar, Cold Regions Science and Technology, 38, 55–61, doi:10.1016/j.coldregions.2003.08.002, URL https://www.sciencedirect.com/science/article/pii/S0165232X03001022, 2004.

Jenssen, R. O. R. and Jacobsen, S.: Drone-mounted UWB snow radar: technical improvements and field results, Journal of Electromagnetic Waves and Applications, 34, 1930–1954, doi:10.1080/09205071.2020.1799871, URL https://doi.org/10.1080/09205071.2020.1799871, 2020.

Jenssen, R. O. R., Eckerstorfer, M., Vickers, H., Høgda, K.-A., Malnes, E., and Jacobsen, S. K.: Drone-Based UWB Radar to Measure Snow Layering in Avalanche Starting Zones, in: International Snow Science Workshop 2016 Proceedings, Breckenridge, CO, USA, pp. 573–577, Breckenridge, CO, USA, URL https://arc.lib.montana.edu/snow-science/item.php?id=2325, 2016.

Jenssen, R. O. R., Eckerstorfer, M., and Jacobsen, S.: Drone-Mounted Ultrawideband Radar for Retrieval of Snowpack Properties, IEEE Transactions on Instrumentation and Measurement, 69, 221–230, doi:10.1109/TIM.2019.2893043, 2020.

Keuschnig, M.: Die Anwendung von Georadar auf Lawinenablagerungen, Masterarbeit, Universität Salzburg, Salzburg, 2010.

Lei, W., Hou, F., Xi, J., Tan, Q., Xu, M., Jiang, X., Liu, G., and Gu, Q.: Automatic hyperbola detection and fitting in GPR B-scan image, Automation in Construction, 106, 102 839, doi:10.1016/j.autcon.2019.102839, URL https://www.sciencedirect.com/science/article/pii/S0926580519301347, 2019.

Li, Y., Zhao, Z., Luo, Y., and Qiu, Z.: Real-Time Pattern-Recognition of GPR Images with YOLO v3 Implemented by Tensorflow, Sensors (Basel, Switzerland), 20, 6476, doi:10.3390/s20226476, URL https://www.ncbi.nlm.nih.gov/pmc/articles/PMC7696763/, 2020.

Lundberg, A., Richardson-Näslund, C., and Andersson, C.: Snow density variations: consequences for ground-penetrating radar, Hydrological Processes, 20, 1483–1495, doi:10.1002/hyp.5944, URL https://onlinelibrary.wiley.com/doi/abs/10.1002/hyp.5944, 2006.

McGrath, D., Webb, R., Shean, D., Bonnell, R., Marshall, H.-P., Painter, T. H., Molotch, N. P., Elder, K., Hiemstra, C., and Brucker, L.: Spatially Extensive Ground-Penetrating Radar Snow Depth Observations During NASA's 2017 SnowEx Campaign: Comparison With In Situ, Airborne, and Satellite Observations, Water Resources Research, 55, 10 026–10 036, doi:10.1029/2019WR024907, 2019.

Prager, S., Sexstone, G., McGrath, D., Fulton, J., and Moghaddam, M.: Snow Depth Retrieval With an Autonomous UAV-Mounted Software-Defined Radar, IEEE Transactions on Geoscience and Remote Sensing, 60, 1–16, doi:10.1109/TGRS.2021.3117509, 2022.

Sand, K. and Bruland, O.: Application of Georadar for Snow Cover Surveying: Paper presented at the 11th Northern Res. Basins Symposium/Workshop Prudhoe Bay to Fairbanks, Alaska, USA – Aug. 18-22, 1997, Hydrology Research, 29, 361–370, doi:10.2166/nh.1998.0026, URL https://doi.org/10.2166/nh.1998.0026, 1998.

Schmid, L., Heilig, A., Mitterer, C., Schweizer, J., Maurer, H., Okorn, R., and Eisen, O.: Continuous snowpack monitoring using upward-looking ground-penetrating radar technology, Journal of Glaciology, 60, 509–525, doi:10.3189/2014JoG13J084, 2014.

Schmid, L., Koch, F., Heilig, A., Prasch, M., Eisen, O., Mauser, W., and Schweizer, J.: A novel sensor combination (upGPR-GPS) to continuously and nondestructively derive snow cover properties: Snow measurements with upGPR-GPS, Geophysical Research Letters, 42, 3397–3405, doi:10.1002/2015GL063732, URL http://doi.wiley.com/10.1002/2015GL063732, 2015.

Schweizer, J., Bartelt, P., and van Herwijnen, A.: Snow avalanches, in: Snow and ice-related hazards, risks and disasters, pp. 395–436, Elsevier, Amsterdam, URL https://www.dora.lib4ri.ch/wsl/islandora/object/wsl%3A12141/, 2015.

Valence, E., Baraer, M., Rosa, E., Barbecot, F., and Monty, C.: Drone-based ground-penetrating radar (GPR) application to snow hydrology, The Cryosphere, 16, 3843–3860, doi:10.5194/tc-16-3843-2022, URL https://tc.copernicus.org/articles/16/3843/2022/, 2022.

Wang, S., Leng, Z., Zhang, Z., and Sui, X.: Automatic asphalt layer interface detection and thickness determination from ground-penetrating radar data, Construction and Building Materials, 357, 129 434, doi:10.1016/j.conbuildmat.2022.129434, URL https://www.sciencedirect.com/science/article/pii/S0950061822030902, 2022.

Wunderlich, T., Wilken, D., Majchczack, B. S., Segschneider, M., and Rabbel, W.: Hyperbola Detection with RetinaNet and Comparison of Hyperbola Fitting Methods in GPR Data from an Archaeological Site, Remote Sensing, 14, 3665, doi:10.3390/rs14153665, URL https://www.mdpi.com/2072-4292/14/15/3665, 2022.